J Mater Sci: Mater Med (2013) 24:1285–1292
DOI 10.1007/s10856-013-4876-7

Evaluation of early stage human bone marrow stromal proliferation, cell migration and osteogenic differentiation on μ-MIM structured stainless steel surfaces

Malak Bitar · Fausta Benini · Claudia Brose · Vera Friederici · Philipp Imgrund · Arie Bruinink

Received: 23 July 2012 / Accepted: 21 January 2013 / Published online: 6 February 2013

Abstract It is well established that surface topography greatly affect cell—surface interactions. In a recent study we showed that microstructured stainless steel surfaces characterized by the presence of defined hexagonally arranged hemisphere-like structures significantly affected cell architecture (shape and focal adhesion size) of primary human bone mesenchymal stromal cells. This study aimed at further investigating the influence these microstructures (microcline protruding hemispheres) on critical aspects of cell behaviour namely; proliferation, migration and osteogenic differentiation. As with previously reported data, we used primary human bone mesenchymal stromal cells to investigate such effects at an early stage in vitro. Cells of different patients were utilised for cell migration studies. Our data showed that an increase in cell proliferation was exhibited as a function of surface topography (hemispheres). Cell migration velocity also varied as a function of surface topography on patient specific basis and seems to relate to the differentiated state of the seeded cell population (as demonstrated by bALP positivity). Osteogenic differentiation, however, did not exhibit significant variations (both up and down-regulation) as a function of both surface topography and time in culture.

Electronic supplementary material The online version of this article (doi:10.1007/s10856-013-4876-7) contains supplementary material, which is available to authorized users.

M. Bitar · F. Benini · C. Brose · A. Bruinink (✉)
Materials-Biology Interactions Lab, EMPA, Lerchenfelstrasse 5, 9014 St. Gallen, Switzerland
e-mail: arie.bruinink@empa.ch

Present Address:
M. Bitar
Technical Research and Development, Novartis Pharma AG, 4057 Basel, Switzerland

V. Friederici · P. Imgrund
Fraunhofer Institute for Manufacturing and Advanced Materials (IFAM), Wiener Strasse 12, 28359 Bremen, Germany

1 Introduction

Due to excellent mechanical properties, corrosion resistance and biocompatibility, stainless steel is widely used to produce bone fixation devices at a relatively low cost [1]. The main disadvantage of using stainless steel, however, lies in reduced osteogenic bioactivity compared to titanium alloys as the gold standard material destined for osteointegration devices. Following implantation, stainless steel implants will become surrounded by a fibrous capsule rather than direct bone-implant contact interface [2]. Surface topography modification may lead to corresponding changes in behaviour upon adherence to these surfaces. Such a changes may greatly influence gene expression and subsequently induce osteogenic differentiation in the contacting cells [3–7]. Relevant surface topography surface functionalization may include roughening, patterning (cell adhesive islands within a cell repellent surface, e.g. [8]) or by microstructuring [7]. For instance, groove and ridge surface structuring was reported to alter cell shape, functionality and migration velocity [9, 10]. Furthermore, Schneider and co-workers showed that groove microtopography enhanced osteogenic differentiation in human embryonic palatal mesenchymal cells [11]. Similarly, Liao and co-workers showed that surfaces exhibiting dense array of 32 μm sized pyramids stimulated rat calvarial osteoblast differentiation independent of the surface chemistry (hydrophobic or hydrophilic) [12] suggesting that indeed by microstructuring unfavourable surfaces can be changed in osteogenesis promoting surfaces. Recently, we

demonstrated that a 316L stainless steel surfaces bearing a defined array of reproducible micrometer scale protruding hemisphere like structures, produced by a micro metal injection moulding technology [13], evoked not only a change in cell shape but also a significant increase of focal adhesion (FA) size [14]. In this respect, it has been suggested that a correlation exists between FA area size, cell differentiation and migration velocity, and between cell shape and cell differentiation [4, 15–19].

This study further evaluated the influence of stainless steel based, hemisphere functionalised (termed as 30_20 and 50_20 surfaces), on cell functionality taking cell proliferation, osteogenic differentiation and cell motility velocity as indicators. These surfaces were produced using an optimised micron metal injection process showing a great potential for scaled-up, topography incorporated, orthopaedic implants [20]. The bioactivity of such hemisphere structured surfaces were compared to that of non-microstructured (NS), plane, surfaces produced via the similar process, baring similar submicrometer scale surface roughness and of similar chemical characteristics (i.e. 316L stainless steel).

The data obtained in this study suggested that the presence of the hemisphere arrays resulted in reduced cell proliferation behaviour compared to that on the non-structured surfaces. Osteogenic differentiations, however (up to 2 weeks in vitro), as indicated by collagen I, osteocalcin and alkaline phosphatase (bALP), were not promoted as function of surface functionalization. Patient specific, cell migration velocity, showed an increase for two of the cell populations investigated in this study. This appeared to correspond to initial state of cell population osteogenic (bALP) protein expression.

2 Materials and methods

2.1 Sample preparation

Biocompatible structured square (8 × 8 mm, 1.5 mm height) and circular samples (d = 9, 2 mm height) were prepared using the optimised Micro metal injection moulding (μ-MIM)process as previously described [13, 14].Briefly, the surfaces were prepared bymixing 33.3 % of master alloy powder with D_{50} size of 3.6 μm and D_{90} of 5.8 μm (Sandvik Osprey Ltd., UK), 66.7 % of nanosized (D_{50} = 0.02 μm, D_{90} = 2.0 μm; American Elements Ltd., USA) Carbonyl iron powder. After sintering, the 316L stainless steel surfaces were composed of a reproducible array of hemispheres. As previously described, the material exhibited fully austenitic characteristics (Cr 18.64 %,Ni 12.28 %, Mo 2.36 %, C0.0310 ± 0.0026 %) in line with the ASTM standard (Cr 16.5–18.5 %, Ni10–13 %,Mo 2–2.5 %, C < 0.0300 %). Three surface variants were produced, (i) plane with no surface microtopography, (ii) surfaces bearing hemisphere arrays of 30.0 ± 0.2 μm hemisphere diameter (Fig. 1a), 12.1 ± 0.1 μm hemisphere height and 17.2 ± 0.3 μm interspacing distance termed 30_20 and (iii), surfaces bearing hemisphere arrays of 46.4 ± 0.6 μm hemisphere diameter, 26.4 ± 0.6 μm hemisphere height and 18.5 ± 0.2 μm interspacing distance termed 50_20 surface (sizes are mean ± 1SD). An example of a 50_20 surface is presented in Fig. 1a. Generally, and regardless of the microstructure characteristics (i.e. hemispheres) all surfaces were characterised by the presence of a sub-structural face roughness (Sa) of 410 ± 50 nm as a result of grain formation. The chemical and physical characteristics together with the cytocompatibility of these surfaces are extensively previously described elsewhere [14, 21]. Prior to cell culture experiments, the samples were incubated in 0.05 % Trypsin/EDTA for 15 min at 37 °C and washed with double distilled water to remove adherent organic contaminants and, subsequently, incubated in 70 % ethanol for 20 min. Following the total evaporation of the aspirated ethanol, the samples were cleaned by plasma exposure (Harrick, Plasma PDC-32G, USA)for 2 min at 2 mbar air pressure to further remove any remaining organic contamination. Sterilized surfaces were incubated in α-minimum essential medium (α-MEM) supplemented with 10 % foetal calf serum (FCS) and 1 % 100XPenicillin–streptomycin (PSN)(all from Invitrogen, Basel, Switzerland) at 37 °C for at least 1 h. This preconditioning procedure allows for protein adsorption on the samples and enhances initial cell attachment to the surface.

2.2 Primary human bone marrow stromal cell (HBMC) culture

Adult human bone marrow stromal cells (HBMC) were individually isolated from marrow tissue samples of patients of both sex in the range of 60–90 years old undergoing total hip arthroplasty after informed consent (ethical approval EKSG 08/014) as described [14]. For each experiment, cells of a separate patient were used. Of the resulting HBMC suspension 1.0 × 10^7 cells were seeded into T75 culture flasks in proliferation medium (α-MEM supplemented with 10 % FCS, 1 % PSN and 1 ng/ml Fibroblast growth factor (FGF-2) (Sigma–Aldrich, Buchs, Switzerland).Flasks were kept under cell culture conditions (humidified atmosphere of 95 % air/5 % CO_2 at 37 °C). The medium was replaced twice a week. Cells were harvested at 70–80 % subconfluency (normally after 3–4 weeks in culture). Only cells of passage 1 were used for the experiments. Cell–surface interactions experiments took place in osteogenic medium (OM) consisting of α-MEM with 10 % FCS, 1 % PSN, 50 μM ascorbic acid phosphate and 2 mM β-glycerophosphate with or without10 nM dexamethasone (OM+ and

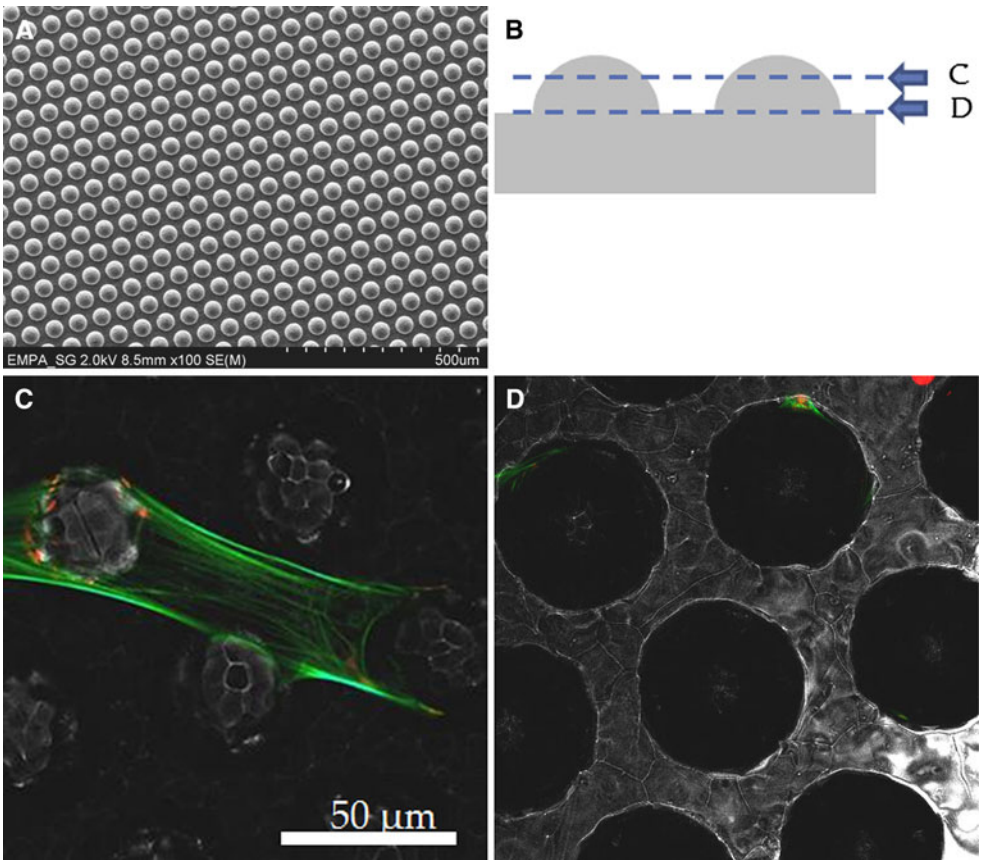

Fig. 1 **a** confocal laser scanning microscope picture of the 30_20 surface used in this study before cell seeding. **b** schematic drawing of a side view of surface with the two planes at which in figure (**c**) and (**d**) CLSM pictures of the same magnification and location of HBMC cells cultured for 7 days were taken. Cells were stained for actin (*green*) and vinculin (*red*). Please note that most vinculin is found on the hemispheres and not on the surface between the hemispheres (Color figure online)

OM−, resp. as mentioned in the text)(the last 3 compounds were all from Sigma–Aldrich). Cells were seeded at 2.5×10^3 cell/cm^2. Seeded samples were kept in 24 well plates with 2 cm^2 well bottom and a 1 ml medium was replaced at 2 day intervals.

2.3 Cell attachment and spreading

The exact location of the cells on the structures was evaluated after 7 days in culture in OM−. Cell staining for attachment and spreading was performed as previously described [14]. Thereafter, cells were evaluated using a confocal laser scanning microscope (Carl Zeiss MicroImaging, Oberkochen, Germany).

2.4 Cell proliferation

Proliferation and total cell number of HBMC kept in OM+ were assessed at days 1 and 7 in vitro as a function of topography. Evaluation of cell proliferation was conducted using the bromdesoxyuridin (BrdU) assays to detect selectively proliferating cells. For this medium was replaced by medium containing 10 µM BrdU (Sigma–Aldrich, Germany). After an additional 14 h under cell culture conditions cells were fixed in 70 % (v/v) ice cold methanol for 20 min at RT and subsequently washed with 0.5 % BSA (Sigma–Aldrich, USA)/PBS. The DNA was later denaturized by incubation in 2 M HCl for 20 min at RT to facilitate BrdU antibody binding. Samples were extensively washed with PBS to ensure total HCl removal and incubated in primary mouse anti-BrdU antibody (clone 347580, BD Biosciences, USA, 1:100 concentration) labelling solution(PBS containing 0.5 % Tween-20 and 0.5 % BSA) for 24 h and at 4 °C. Prior to application of the secondary antibody, the samples were washed with 0.5 % BSA/PBS. Thereafter, samples were incubated in goat anti-mouse IgG (Alexa 488, clone A11029, Invitrogen, USA, 1:400 concentration) secondary antibody solution containing 1:500 concentration of diamidinophenylindol (DAPI) as a DNA stain for 20 min at RT in order to assess total cell number.

Fluorescence imaging took place across the entire seeded/labelled surface for each specimen. For each seeded surface, 30 microscope fields were imaged using an Axio Cam MRm microscope (Zeiss) to obtain both, BrdU

(λ Ex/Em: 488/519 nm) and DAPI (λ Ex/Em: UV/461 nm) labelled nuclei. BrdU positive and total cell numbers (DAPI labelled) were assessed ImageJ image analysis software (version 1.41c, NIH, USA, http://rsb.info.nih.gov/ij/). Proliferation ratio was expressed as the mean for 3 samples calculating the ratio of BrdU positive to total cell number per surface.

2.5 Cell migration and bALP expression

Following cell harvest, the cell population was resuspended in 1 ml α-MEM with 10 % FCS, 1.56 % ethanol and 0.04 % (w/v) dioctadecylindodicarbocyanine iodide (DiI, Fluka, CH) for 15 min at 37 °C for vital labelling. The cells were later washed twice using α-MEM with 10 % FCS by centrifugation (3 min at 94 g) and thereafter seeded onto the various surfaces at 2.5×10^3 cells/cm^2 cell density in OM+.

At the appropriate time points (days 1 and 7 in culture), three seeded surface variants were placed together in a flow chamber equipped with a transparent microscopy viewing cover. The seeded surfaces were immersed in preconditioned tissue culture medium (incubated under cell culture conditions to ensure CO_2 diffusion), the flow chamber sealed and immediately mounted onto fixed onto air heated confocal laser scanning microscope stage at 37 °C (LSM 510, Zeiss, Germany). For each surface, 10 microscope fields were chosen imaged (λ Ex/Em: 543/605 nm) at 15 min intervals, using 20× objective lens for 14 h. Cell trajectories (Fig. 2) were obtained by conversion of the time-lapse image sequences using image analysis software IPS 1.084 and Trace 1.023 (Visiometric, Germany). Cells' centroids coordinates were acquired with IPS, with an intensity thresholds from 50 to 255 and object recognition from 10^2 to 10^6 pixels (Fig. 1). These individual coordinates were listed as x- and y-coordinates to trajectories. Cell trajectories not occurring within the total monitoring time (i.e. cells moving in and out of the microscope filed) or of merging and splitting cells were excluded. Per experiment and surface in average 116 cells (minimal 41, maximal 230) were traced. To account for possible inaccuracies arising from the microscope stage instability, and subsequently interfering with trajectory tracing, auto fluorescing reference points were identified for each time-lapse image sequence. Cell trajectories were later normalised against the corresponding reference points. The corrected trajectories values of x- and y-coordinates at each time-laps frame, i.e. every 15 min, were used to establish cell migration velocities, taking the observed translocation per time frame and 15 min as migration velocity. For each traced cell, median migration velocity was calculated and used for further analysis (frequency pattern and mean migration velocity over the cells per experiment). Each imaged field coordinates were registered so that the exact field was examined following immunocytochemistry labelling in order to correlate cell migration pattern to the osteogenic differentiation state as expressed by bALP expression. Following time lapse examination, the cultures were removed from the flow cells and immediately fixed by direct transfer into 2 % paraformaldehyde and incubated for 10 min and washed with PBS. To reduce non-specific binding samples were incubated for 30 min at room temperature (RT) in 5 % goat serum solution. Thereafter, the samples were incubated in mouse anti-human bone specific alkaline phosphatase (bALP) antibody (clone B4-78, R&D systems, USA; 1:1000 in 1.5 % (w/v) milk powder/PBS solution) for 60 min at RT. After triple washing with PBS, the samples were incubated for 60 min at RT with the secondary goat anti-mouse IgG (Alexa Flour 488, Invitrogen, USA, 1:400 in 1.5 % (w/v) milk powder/PBS solution). CLSM images of the cultures were made (λ Ex/Em: 488/519 nm). Staining of actin using Alexa Fluor® 488 phalloidin, vinculin using Alexa Fluor® 546 labelled second antibody and cell nuclei with BOBO™-1 iodide were performed as previously described[14].

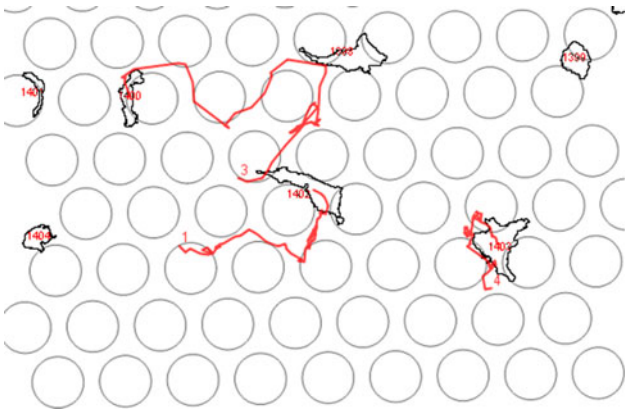

Fig. 2 The 50_20 surface showing a *hexagonal array of hemispheres* and the seeded cell trajectories at day 7 in culture. These trajectories were later numerically expressed and velocities

2.6 Quantitative RT-PCR and alizarin staining

In 3–5 independent experiments mRNA was harvested after 7 and 14 days in culture order to investigate the capacity of the microstructured in inducing osteoblast differentiation of HBMC relative to planar μMIM produced surfaces, Per time point, patient and material mRNA of 3 samples were pooled for quantitative bALP, collagen-I and osteocalcin (OC) mRNA (GeneBank accession numbers NM_000478, NM_000088 and NM_199173, respectively). Assessment was done according [22]. 18S ribosomal RNA (GeneBank accession number NR_003286) was used as normalization standard. In addition to mRNA measurements calcium deposition was assessed by alizarin-red and quantified as

described by Stanford and co-workers after 21 days in culture [23]. Cultures kept on tissue culture plastic in OM− and OM+ were taken as a negative and positive references.

2.7 Statistical evaluation

Where applicable, statistical evaluation (descriptive, non-parametiric) and frequency distribution (relative) was conducted using KyPlot statistical Package (v 2.0 Beta). Non-parametric multiple comparisons were conducted for both cell proliferation and cell migration data as a function of surface topography and time in culture using Tukey-equivalent method at $P < 0.05$ significance level. Cell proliferation data were pooled. For cell migration data, each cell population (patient) was evaluated individually since the migration velocity were correlated to the state of the culture differentiation. Student t test evaluation was conducted to evaluated significant differences in gene expression and alizarin red values as a function of surface topography (compared to NS surfaces).

3 Results

3.1 Cell adhesion and proliferation

As illustrated in Fig. 1c, d at day 7 in OM- medium, HBMC's were well spread on all the surfaces evaluated in this study as expected. Additionally, on the structured surfaces, the seeded cells were predominantly contacting the hemisphere bodies (Fig. 1).

Total cell number, at 24 h in culture, was comparable at all surfaces (Fig. 3). By day 7 in culture however, significant decrease in cell number appeared associated with the structured 30_20 and 50_20 surfaces despite an overall all, time related, increase on all surfaces. BrdU rates as index of proliferating cells exhibited significant decline as a function of time in culture indicating an overall inhibition of cell proliferation (Fig. 4). However, BrdU rates were significantly higher in relation to the 30_20 surfaces by day 7.

3.2 Cell migration and bALP expression

Comparing the migration velocities at day 7 in culture as a function of surface topography, significant increase in velocity value was evident for two patient populations and associated with the 30_20 and 50_20 surfaces compared to the non-microstructured, NS surfaces (Fig. 5 and supplementary data fig. S1). The third patient population evaluated in this study showed an almost reversed trend with cells seeded on the 50_20 surfaces whereby a significant decline in cell velocity was confirmed at both time points

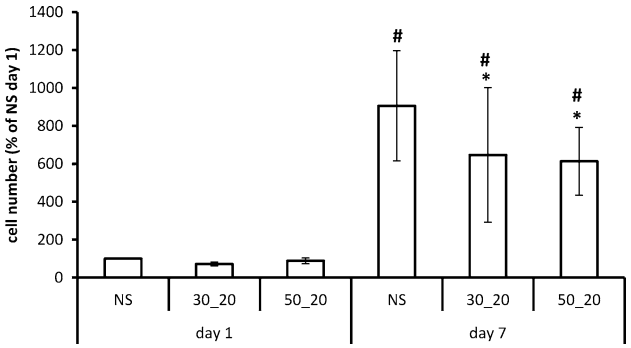

Fig. 3 Cell number at 24 h and 7 days after seeding on NS, 30_20 and 50_20 surfaces. *Bars* represent mean ± S.E.M over 3 independent experiments. * $P < 0.05$ compared with NS of the same day # $P < 0.05$ compared with the same surface at day 1 (t test)

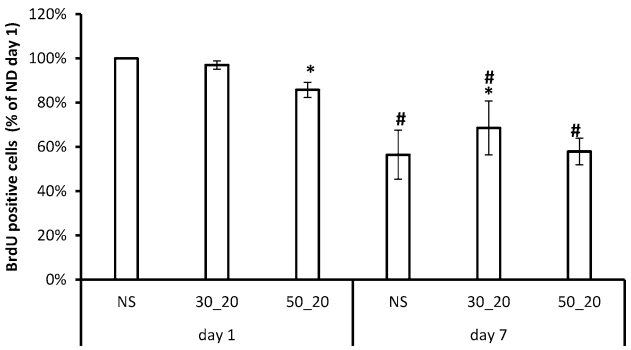

Fig. 4 Percentage of BrdU positive cells on different surfaces after 24 h and 7 days after seeding relative to NS day 1. At day 1, 62 % of the HBMC on NS surfaces were BrdU positive. *Bars* represent mean ± S.E.M over 3 independent experiments. * $P < 0.05$ compared with NS of the same day # $P < 0.05$ compared with the same surface at day 1 (t test)

in culture. Remarkably, (See Fig. 6) HBMC of patient 3 exhibited an early onset of osteogenic differentiation as demonstrated by bALP positivity. Such level was not seen in case of cells of patients 1 and 2, showing elevated migration velocity at 24 h in culture. HBMC of patient 1 and 2 also exhibited comparetively less bALP positive cells at day 7.

3.3 Cell differentiation

mRNA analysis of the cultures kept for 7 or 14 days on the various samples revealed no significant differences in ALP (except NS on day 14), collagen-I and osteocalcin regulation as a function of both, the surface topography and time in culture (Fig. 7). The corresponding mineralisation capacity was also investigated by day 21 in culture. As seen in Fig. 8, cells were able to deposit mineralised matrix in the absence of dexamethasone on these surfaces, however, the presence of the hemispheres did not appear to increase this deposition. The osteogenic potential of the cells used in this study was confirmed by the cell

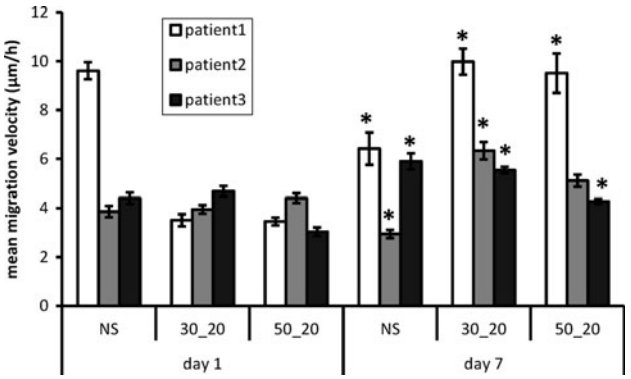

Fig. 5 Mean migration velocity over the median velocity values of the evaluated cells on NS, 30_20 and 50_20 surfaces. Mean values (± S.E.M.) of cells of each of the 3 patients are presented. The migration velocity distribution is shown in supplementary data Fig. S1. *$P < 0.05$ as a function of surface topography at each time point

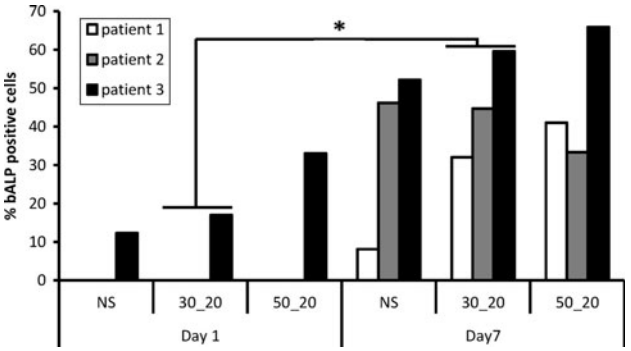

Fig. 6 The percentage of bALP positive cells in HBMC cultures after 24 h and 7 days in culture on NS, 30_20 and 50_20 surfaces (feedstock I) of each patient separately. Please not that on day 1 no positive bALP cells were found in case of patient 1 and 2. Data represent mean S.E.M. over x cells. # $P < 0.05$ compared with the same surface at day 1 (t test, $n = 3$)

population ability to react with significantly enhanced mineralisation capacity as result of the addition of dexamethasone (data not shown).

4 Discussion

This study evaluated HBMC behaviour upon seeding on stainless steel microstructured surfaces composed of a reproducible array of hemispheres (Figs. 1 a, b). The parameters evaluated in this study were related to the influence that these surfaces exerted on cell proliferation, migration and the induction of osteogenesis as a function of both, time in culture and structure parameters (i.e. hemisphere dimensions and their presence). We aimed at further evaluating the osteogenic potential of hemisphere based surface functionalization whereby stainless steel material may be utilised as long lasting, osteointegrated, devices.

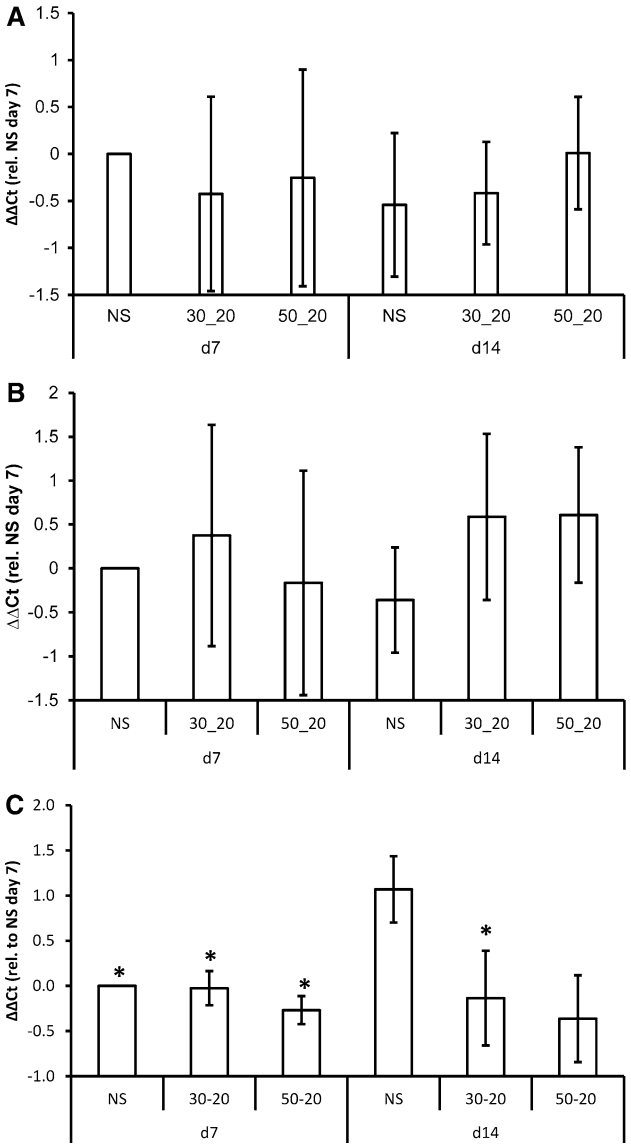

Fig. 7 Effects of surface microstructuring on HBMC differentiation taking gene expression in HBMC cultures as an index. HBMC were kept for 7 and 14 on NS, 30_20 and 50_20 surfaces: Collagen-I (**a**), osteocalcin (**b**) and ALP (**c**). *Bars* represent mean ± S.E.M over 3 (osteocalcin) or 5 (collagen-I, ALP) independent experiments relative to cultures kept on NS surface after 7 days in culture. Negative ΔΔCt values stand for a relative increase of the m-RNA values relative to NS day 7 controls. * $P < 0.05$ significant different from NS day 14 comparing raw Ct values (t test)

Previously, we reported that these stainless steel based microstructures significantly affected cell morphology and resulted in a significant ~20 % increase of focal adhesion size as measured after 7 days in culture compared to their non-structured equivalent [14]. In this study, we also aimed at correlating our finding to our previous report.

Zinger and his colleagues observed that on titanium surfaces with surface pattern similar as presented here but inverse (also with a submicrometer roughness) cell number of MG63 osteoblasts was decreased by the microstructures

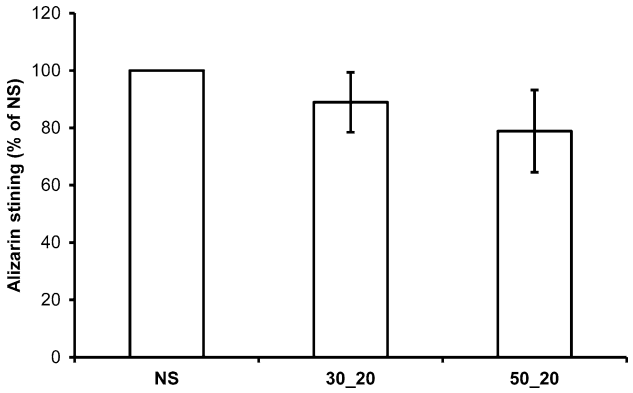

Fig. 8 Effects of surface microstructuring on mineralisation of the HBMC cultures 21 days after seeding taking alizarin-red concentration after staining as an index. * $P < 0.05$ compared with HBMC cultures on TCPS kept in osteogenic medium with dexamethasone. *Bars* represent mean ± S.E.M over 8 independent experiments

as measured 5 days after seeding [24]. In this study, all cultures underwent an overall significant decline of cell proliferation on all surface variants by day 7 in culture. This may be related to both contact inhibition and/or the activation of differentiation pathways of the cells (e.g. [25, 26]). Overall cell number ratios, on the other hand and irrespective of proliferation rates, were significantly lower on the structured surfaces possibly indicating topography effect in line with cell shape and focal adhesion modulation induced by these surfaces [14]. We do not expect that the decline in cell number relate to cell viability (survival) on these surfaces [14].

As previously found, after 7 days in culture cells adhered well on all surfaces but on the microstructured surfaces FA were specifically located on the hemispheres. Their size was significantly increased [14]. Rodriguez-Fernandez and co-workers described that cell motility is increased after application of a vinculin antisense construct. The transfected cells exhibited a rounded phenotype with less vinculin-positive FAs. [27]. On the other hand by increasing the expression of vinculin cell adhesion was found to be promoted and cell motility reduced [19]. Recently, it was also described that differentiation of HBMC towards osteoblast is correlated with a reduction of cell area increase in compactness and an elongation of cells [7]. Likewise, a positive correlation seems to exist between cell differentiation and migration as reported for adult mesenchymal stem cells differentiation towards myoblasts [28]. By combining migration data of 3 patients we could not find an overall effect of the microstructures on cell migration velocity. Correlating the finding of this study (cell migration velocity) with our previous study (cell shape and FA size), no direct correlation may statistically be proven whereby, ultimately, a confirmed potential induction of specific differentiation pattern may not be associated with 30_20 and 50_20 surfaces. This may be related to the heterogeneity of differentiation potential of HMBC of each specific patient.

To verify the increased osteogenic potential of the hemisphere structures, we evaluated osteogenic gene expression in the mid-term (1–2 weeks in culture). For this HBMC were cultured in osteogenic medium without dexamethasone in order to detect minor differentiation promoting effects which else might be overruled by the strong differentiation stimulating effects of dexamethasone [29–32]. Based on ALP, collagen-I and osteocalcin mRNA measurements after 7 and 14 days in culture as well as on calcium deposition after 21 days in culture no effects of the microstructures on differentiation could be detected. Thus, in contrast to the general accepted rule it seems that a significant change in cell shape, an increase in FA size and reduction of cell proliferation may, but need not, influence cell differentiation, i.e. that no causality between these parameters exist. Here, Engel and co-workers were not able to correlate cell shape and the expected state of differentiation. They evaluated the effect of ring-like ridges (ring diameter 50 μm) on rat bone marrow stromal cells where no specific effect on cell proliferation and differentiation took place despite clear, corresponding, induction of cell morphology conformation [33]. It might be hypothesized that by using different substratum chemistry such causal relationship may indeed take place. The material investigated in this study, 316L stainless steel, does not support osteointegration by default.

In conclusion, the present study revealed that surfaces structuring of stainless steel characterized by regular array of micrometer scaled, equally spaced, hemispheres resulted in an overall reduction in HBMC proliferation, however, osteogenic differentiation was not induced compared to non-structured surfaces. Cell migration patterns were altered in relation to the presence of the hemispheres however, this was strongly donor patient based. More impotently, we have demonstrated that the modulation of cell shape (increased elongation) and focal adhesion nature (increased size) as previously reported may not linked to a reduction in migration velocity and promotion of a specific differentiation state—here, both experimental patient related population heterogeneity and surface chemistry (Stainless Steel) may overcome surface topography.

Ultimately, we aim at further investigating these surfaces whereby both topography (further size variations) and chemistry (Alloy variations) may lead to a universal induction of osteogenic differentiation of HBMC's regardless of patient related variations.

Acknowledgments The authors acknowledge the generous support of the Volkswagen Foundation (contract nr. 182–296) in Germany.We also thank Kantonsspital St. Gallen (CH) for providing the human tissue samples.

References

1. Disegi JA, Eschbach L. Stainless steel in bone surgery. Inj Suppl. 2000;4(31):2.
2. Lee M-H, Park I-S, Min K-S, et al. Evaluation of in vitro and in vivo tests for surface–modified titanium by H_2SO_4 and H_2O_2 treatment. Met Mater Int. 2007;13:109.
3. Shannon JM, Pitelka DR. The influence of cell shape on the induction of functional differentiation in mouse mammary cells in vitro. In Vitro. 1981;17:1016.
4. Watt FM, Jordan PW. CH O'Neill cell shape controls terminal differentiation of human epidermal keratinocytes. Proc Natl Acad Sci USA. 1988;85:5576.
5. Boone C, De Clercq L, Grégoire F, Remacle C. The modulation of cell shape influences porcine preadipocyte differentiation. In Vitro Cell Dev Biol. 1999;35:61.
6. Takagi M, Kitabayashi K, Koizumi S, et al. Correlation between cell morphology and aggrecan gene expression level during differentiation from mesenchymal stem cells to chondrocytes. Biotechnol Lett. 2008;30:1189.
7. Unadkat HV, Hulsman M, Cornelissen K, et al. An algorithm-based topographical biomaterials library to instruct cell fate. Proc Natl Acad Sci USA. 2011;108:16565.
8. Kilian KA, Bugarija B, Lahn BT, Mrksich M. Geometric cues for directing the differentiation of mesenchymal stem cells. Proc Natl Acad Sci USA. 2010;107:4872.
9. Kaiser J-P, Bruinink A. Investigating cell-material interactions by monitoring and analysing cell migration. J Mater Sci Mated Med. 2004;15:429.
10. Bruinink A, Wintermantel E. Grooves affect primary bone marrow but not osteoblastic MC3T3-E1 cell cultures. Biomaterials. 2001;22:2465.
11. Schneider GB, Zaharias R, Seabold D, Keller J, Stanford C. Differentiation of preosteoblasts is affected by implant surface microtopographies. J Biomed Mater Res. 2004;69A:462.
12. Liao H, Andersson AS, Sutherland D, Petronis S, Kasemo B, Thomsen P. Response of rat osteoblast-like cells to microstructured model surfaces in vitro. Biomaterials. 2003;24:649.
13. Imgrund P, Bitar M, Friederici V, Bruinink A (2012) Scripta Materialia (in preparation).
14. Bitar M, Friederici V, Imgrund P, Brose C, Bruinink A. In vitro bioactivity of micro metal injection moulded stainless steel with defined surface features. Eur Cell Mater. 2012;23:333.
15. Born A-K, Rottmar M, Lischer S, Pleskova M, Bruinink A, Maniura-Weber K. Correlating cell architecture with osteogenesis: first steps towards live single cell monitoring. Eur Cell Mater. 2009;18:49.
16. Li F, Wang Q-M, Wang JH-C. Cell shape regulates collagen type I expression in human tendon fibroblasts. Cell Motil Cytoskeleton. 2008;65:332.
17. McBeath R, Pirone DM, Nelson CM, Bhadriraju K, Chen CS. Cell shape, cytoskeletal tension, and RhoA regulate stem cell lineage commitment. Dev Cell. 2004;6:483.
18. Lamers E, van Horssen R, te Riet J, et al. The influence of nanoscale topographical cues on initial osteoblast morphology and migration. Eur Cell Mater. 2010;9:329.
19. Rodríguez Fernández JL, Geiger B, Salomon D, Ben-Ze'ev A. Overexpression of vinculin suppresses cell motility in BALB/c 3T3 cells. Cell Motil Cytoskeleton. 1992;22:127.
20. Imgrund P, Rota A, Simchi A. Microinjection moulding of 316L/17-4PH and 316L/Fe powders for fabrication of magnetic-non-magnetic bimetals. J Mat Process Technol. 2008;200:259.
21. Imgrund P, Schmidt H, Salk N, Bruinink A, Bitar M. Metal Powder Industries Federation. In: Lawcock R, Lawley A, McGeehan PJ (eds) Advances in Powder Metallurgy & Particulate Materials-2008. New Jersey, Washington DC, 2008.
22. Born A-K, Lischer S, Maniura-Weber K. Watching osteogenesis: life monitoring of osteogenic differentiation using an osteocalcin reporter. J Cell Biochem. 2012;113:313.
23. Stanford CM, Jacobson PA, Eanes ED, Lembke LA, Midura RJ. Rapidly forming apatitic mineral in an osteoblastic cell line (UMR 106-01 BSP). J Biol Chem. 1995;270:9420.
24. Zinger O, Zhao G, Schwartz Z, et al. Differential regulation of osteoblasts by substrate microstructural features. Biomaterials. 2005;26:1837.
25. Gu YX, Du J, Si MS, Mo JJ, Qiao SC, Lai HC. The roles of PI3K/Akt signaling pathway in regulating MC3T3-E1 preosteoblast proliferation and differentiation on SLA and SLActive titanium surfaces. J Biomed Biomater Res A. 2013;101:748
26. Lincks J, Boyan BD, Blanchard CR, et al. Response of MG63 osteoblast-like cells to titanium and titanium alloy is dependent on surface roughness and composition. Biomaterials. 1998;19:2219.
27. Rodríguez Fernández JL, Geiger B, Salomon D, Ben-Ze'ev A. Suppression of vinculin expression by antisense transfection confers changes in cell morphology, motility, and anchorage-dependent growth of 3T3 cells. J Cell Biol. 1993;122:1285.
28. Nedeau AE, Bauer RJ, Gallagher K, Chen H, Liu ZJ, Velazquez OC. A CXCL5- and bFGF-dependent effect of PDGF-B-activated fibroblasts in promoting trafficking and differentiation of bone marrow-derived mesenchymal stem cells. Exp Cell Res. 2008;314:2176.
29. Aguilar-Vázquez R, Carballo-Molina OA, Collazo-Navarrete O, et al. Osteogenesis of human vascular endothelial cells in culture. Rev Invest Clin. 2008;60:496.
30. Shui C, Scutt AM. Mouse embryo-derived NIH3T3 fibroblasts adopt an osteoblast-like phenotype when treated with 1alpha,25-dihydroxyvitamin D(3) and dexamethasone in vitro. J Cell Physiol. 2002;193:164.
31. Lavenus S, Pilet P, Guicheux J, Weiss P, Louarn G, Layrolle P. Behaviour of mesenchymal stem cells, fibroblasts and osteoblasts on smooth surfaces. Acta Biomater. 2011;7:1525.
32. Leclerc N, Noh T, Khokhar A, Smith E, Frenkel B. Glucocorticoids inhibit osteocalcin transcription in osteoblasts by suppressing Egr2/Krox20-binding enhancer. Arthritis Rheum. 2005;52:929.
33. Engel E, Martínez E, Mills CA, Funes M, Planell JA, Samitier J. Mesenchymal stem cell differentiation on microstructured poly (methyl methacrylate) substrates. Ann Anat. 2009;191:136.